IJARST

International Journal of Advanced Research in Science and Technology

https://doi.org/10.62226/ijarst20262769

ISSN 2319 – 1783 (Print)
ISSN 2320 – 1126 (Online)

Environment Management Using Nano-Technology

Sanjeev Goyal
Department of AS&H, RKGIT, Ghaziabad
drsgoyalji@gmail.com

ARTICLE INFO

Article history:

Received	04 May 2026
Accepted	17 May 2026
Available online	23 May 2026

Keywords:
Nanomaterials; Environmental Remediation; Photocatalysis; Adsorption; MXenes; Green Nanotechnology; Nano-ecotoxicology; Circular Economy

Indexed in:

Crossref
INDEX COPERNICUS INTERNATIONAL
Google scholar

and in major libraries

ABSTRACT

Global environmental contamination, driven by rapid industrialization, urbanization, and agricultural intensification, represents one of the foremost public health and ecological challenges of the twenty-first century. Nanomaterials—distinguished by their sub-100 nm dimensions, exceptionally high surface-area-to-volume ratios, and precisely tunable surface chemistries—have emerged as a transformative technology platform for pollution abatement across water, soil, and air matrices. This paper presents a rigorous, cross-domain review of nanomaterial-based environmental remediation, encompassing established systems (TiO_2, Fe_3O_4, ZnO, nZVI, carbon nanotubes, graphene oxide, silver nanoparticles, and polymeric nanofibers) alongside next-generation materials including MXenes, covalent organic frameworks (COFs), and quantum dots. Mechanistic pathways—photocatalysis, adsorption, reductive dechlorination, membrane filtration, and antimicrobial action—are elucidated in this paper.

I. INTRODUCTION

Pollution of natural ecosystems has reached an inflection point demanding technological intervention. Roughly 300–400 million tons of heavy metals, solvents, and toxic sludge are discharged into global waterways annually, while atmospheric fine particulate matter ($PM_{2.5}$) accounts for approximately 7 million premature deaths each year according to World Health Organization estimates [1]. Agricultural soils across Southeast Asia and Sub-Saharan Africa carry cadmium, arsenic, and organochlorine pesticide residues at concentrations several times above WHO permissible limits. The inadequacy of conventional treatment technologies—whose removal efficiencies for trace micro pollutants at part-per-billion concentrations are well-documented to fall between 50% and 80%—has created an urgent demand for step-change innovations in remediation science [2].

Nanotechnology, broadly defined as the design and application of materials and structures at the 1–100 nm scale, addresses this challenge directly. At such dimensions, quantum mechanical effects alter electronic band structures, surface free energies reach values orders of magnitude above bulk analogues, and the proportion of surface atoms can approach 50–80% of total atoms—properties that collectively confer extraordinary reactivity, adsorptive capacity, and catalytic performance [3]. These characteristics underpin the rapidly expanding application of nanomaterials in environmental remediation, a field whose research output has grown exponentially—from approximately 3,200 publications in 2018 to over 13,800 in 2026 (Fig. 1).

This paper provides a comprehensive, critically evaluated synthesis of the current state of nanomaterial-based environmental remediation. It introduces a structured classification of nanomaterial types, mechanistic pathways, and target pollutant domains; benchmarks performance quantitatively against conventional technologies; examines next-generation nanomaterial classes not yet covered in prior reviews; and proposes actionable priorities for bridging laboratory-scale advances to sustainable field deployment.

II. BACKGROUND

A. Severity and Scope of Environmental Pollution

Water contamination by heavy metals constitutes one of the most pervasive threats to human and ecosystem health. Lead concentrations in tap water supplying approximately 10 million US households still exceed the EPA action level of 15 µg/L, while arsenic contamination of groundwater affects an estimated 200 million people across Bangladesh, India, Pakistan, and China [4]. Mercury bioaccumulation in marine food chains has elevated methylmercury concentrations in large pelagic fish species to levels that impose measurable neurodevelopmental risks on populations with high levels of fish consumption.

Soil contamination presents a distinct challenge. Recalcitrant organochlorine compounds—DDT, lindane, PCBs—persist for decades in agricultural soils due to their hydrophobicity and resistance to microbial degradation. In industrial zones, polycyclic aromatic hydrocarbons (PAHs) and volatile organic compounds (VOCs) percolate through unsaturated zones to contaminate shallow aquifers. The United States Environmental Protection Agency's Superfund list includes over 1,300 priority contaminated sites, the majority involving multi-contaminant soil and groundwater co-pollution [5].

B. Limitations of Conventional Remediation Technologies

The principal conventional water treatment methods—coagulation-flocculation, sand filtration, activated carbon adsorption, and reverse osmosis—carry well-recognized limitations. Coagulation generates large volumes of metal-hydroxide sludge requiring secondary disposal; activated carbon adsorbs rather than destroys contaminants and requires periodic, energy-intensive thermal regeneration; reverse osmosis consumes 3.5–5.0 kWh/m^3 and produces concentrated brine with limited disposal options. Biological treatment methods, while sustainable in principle, are characteristically slow, with hydraulic retention times of 8–24 hours, and remain vulnerable to toxic shock from industrial effluent loads [5]. These deficiencies—high cost, secondary waste streams, limited micropollutant efficacy—collectively justify the scientific investment in nanomaterial-based alternatives.

C. Historical Development of Environmental Nanomaterials

The intellectual foundations of nanotechnology were established by Richard Feynman's seminal 1959 lecture, "There's Plenty of Room at the Bottom." Iijima's discovery of carbon nanotubes in 1991 [12] and Novoselov and Geim's isolation of graphene in 2004 [14] established two of the most consequential nanomaterial families. For remediation specifically, the TiO_2 photocatalysis pathway was identified by Fujishima and Honda in 1972 [13]—though its environmental applications took another two decades to develop. Zero-valent iron nanoparticles for in-situ groundwater treatment were first reported in the late 1990s and achieved commercial field deployment by 2010, making this the most field-mature nanomaterial remediation technology available. Since 2018, the field has evolved rapidly, with MXenes, COFs, and quantum-dot-based photocatalysts emerging as particularly promising next-generation platforms [11].

III. PROBLEM STATEMENT, OBJECTIVES, AND SCOPE

A. Problem Statement

Despite a growing body of laboratory evidence supporting the efficacy of nanomaterial-based remediation, a critical translation gap persists between bench-scale findings and field deployment. Three interrelated challenges account for this gap. First, the literature remains fragmented by domain—water, soil, and air remediation communities publish largely in separate journals with limited cross-pollination. Second, performance benchmarking lacks standardization: reported removal efficiencies vary considerably with initial contaminant concentration, pH, temperature, ionic strength, and nanomaterial loading, rendering cross-study comparisons unreliable. Third, ecotoxicological data on the fate and long-term effects of remediation nanomaterials in receiving environments remain sparse and inconsistent, generating regulatory uncertainty that has impeded wider adoption.

B. Research Objectives

- To classify and characterise principal nanomaterial platforms used in environmental remediation, including emerging MXene, COF, and quantum-dot systems not addressed in prior reviews.
- To elucidate the mechanistic underpinnings—photocatalysis, adsorption kinetics, reductive dechlorination, membrane filtration—governing pollutant removal, with supporting mathematical formulations.
- To conduct a structured, multi-parameter comparative analysis of nanomaterial performance against conventional remediation technologies across water, soil, and air domains.
- To evaluate green synthesis routes as environmentally responsible nanomaterial production alternatives.
- To identify research gaps in nano-ecotoxicology and regulation, and propose a technology roadmap for responsible, scalable deployment.

C. Scope of Study

This review draws on peer-reviewed literature published between 2018 and 2026, retrieved from the Scopus, Web of Science, and arXiv databases using structured search terms ('nanomaterials environmental remediation,' 'nano-photocatalysis pollution,' 'green synthesis nanoparticles,' and related combinations). The scope intentionally spans all three environmental matrices and encompasses both fundamental mechanistic studies and field or pilot-scale implementations. Techno-economic and regulatory dimensions are addressed qualitatively within the constraints of a review article format.

IV. LITERATURE REVIEW

A. Previous Research Work

Guerra et al. [1] produced a foundational survey of nanotechnology applications in environmental remediation, synthesizing data from over 400 studies and establishing TiO_2, iron oxide, and carbon-based nanomaterials as the three dominant platform families. The review underscored photo catalysis and adsorption as the dominant mechanistic pathways and called for standardized protocols to enable inter-laboratory comparison. This call has remained largely unmet, a gap that this paper directly addresses through its structured comparative tables and multi-parameter analysis.

Asghar et al. [2] applied bibliometric analysis to 1,240 nanomaterial remediation publications between 2010 and 2023, revealing that China (38%), the United States (17%), and India (11%) collectively account for two-thirds of global research output. Their synthesis pathway analysis found hydrothermal routes to be most widely adopted (41% of studies), followed by co-precipitation (29%) and sol-gel (18%). Crucially, only 6% of publications included field-scale or pilot-scale validation data—a finding that directly motivates this paper's emphasis on scalability and field validation.

Yang and Shen [3] reviewed metal and metal-oxide nanoparticles for environmental applications, establishing quantitative performance benchmarks. TiO_2 photocatalysts achieved >95% degradation of methyl orange within 120 minutes under UV irradiation; Fe_3O_4 nanoparticles removed 98.3% of Pb^{2+} at pH 6 and a dosage of 1.0 g/L. The review also highlighted the role of morphology control in tuning photocatalytic efficiency, with anatase-phase TiO_2 nanosheets outperforming spherical particles by 23% for phenol mineralization.

Norton and Norton [4] surveyed inorganic nanomaterials for sustainable water remediation with particular attention to nZVI, documenting that direct-push injection of nZVI suspensions into TCE-contaminated groundwater achieved 99% contaminant reduction within 180 days in field pilots across three US states. Wang et al. [7] conducted a rigorous assessment of carbon nanotube and graphene oxide adsorption thermodynamics, reporting Langmuir monolayer adsorption capacities of 270 mg/g (f-MWCNT) and 310 mg/g (GO) for methylene blue, with adsorption proceeding spontaneously and endothermically ($\Delta G° < 0$; $\Delta H° > 0$).

Atanda et al. [10] raised important ecotoxicological considerations: TiO_2 nanoparticles at concentrations exceeding 1 mg/L impair the reproductive capacity of Daphnia magna by 34% over 21 days, while silver nanoparticles exhibit bactericidal activity at 0.1–1 μg/mL—concentrations that could disrupt natural soil microbial communities essential for nitrogen cycling. The review by Frontiers in Chemistry [11] on next-generation nanomaterials documented MXene-based sorbents achieving 98% arsenic removal within 30 minutes at a loading of 0.5 g/L, outperforming conventional iron adsorbents by a factor of 3.2 on a per-mass basis.

B. Comparison of Existing Methods

Table II (Section VII) provides a systematic cross-comparison of ten remediation methods. The key distinctions are as follows. Conventional methods such as coagulation-flocculation and sand filtration transfer contaminants from one phase to another rather than destroying them, generating secondary waste requiring disposal. Activated carbon adsorption achieves 60–80% removal for dissolved organics but exhibits sharply reduced efficacy for polar micro-pollutants. Reverse osmosis, while achieving >99% rejection for ionic contaminants, consumes 3.5–5.0 kWh/m³ and produces brine at 10–25% of feed volume. By contrast, photocatalytic nanomaterials mineralise organic pollutants to CO_2 and H_2O without secondary waste, nZVI reduces chlorinated solvents in-situ without excavation, and nano-enabled membranes achieve comparable or superior rejection rates to reverse osmosis at 0.5–1.2 kWh/m³ [5].

C. Research Gaps Identified

- No internationally standardised protocol exists for nano-ecotoxicological testing in receiving water environments.
- Field-scale and pilot-scale validation data cover fewer than 8% of published nanomaterial remediation studies.
- Long-term fate, transformation, and persistence of engineered nanoparticles in complex environmental matrices remain poorly characterized.
- Techno-economic assessments comparing nanomaterial life-cycle costs with conventional treatment alternatives are rare.
- Regulatory frameworks in most jurisdictions do not yet include nano-specific provisions for remediation nanomaterial release, monitoring, or disposal.
- MXene, COF, and quantum-dot systems for environmental applications have been studied almost exclusively at laboratory scale with no field-scale data available as of 2026.

Fig. 1: Annual Research Publication Growth in Nanomaterial-Based Environmental Remediation.

V. NANOMATERIAL CLASSIFICATION AND MECHANISTIC FRAMEWORK

A. Metal-Oxide Nanoparticles

Metal-oxide nanoparticles constitute the most extensively investigated class of materials for environmental remediation applications. Among them, titanium dioxide (TiO_2) in the anatase phase holds a bandgap of 3.2 eV, rendering it photoactive under UV irradiation ($\lambda < 388$ nm). When incident photon energy exceeds this threshold, electron-hole pairs are generated in the conduction and valence bands respectively, as described by Eq. (1):

$$TiO_2 + h\nu \rightarrow e^-_{CB} + h^+_{VB}$$
$$h^+ + H_2O \rightarrow \bullet OH + H^+$$
$$e^- + O_2 \rightarrow \bullet O_2^- \rightarrow \bullet OH \text{ (via } H_2O_2\text{)}$$

The •OH radical, with a standard reduction potential of +2.80 V, non-selectively attacks organic pollutant molecules, ultimately mineralizing them to CO_2, H_2O, and inorganic ions. The photocatalytic mechanism is illustrated in Fig. 4 (see single-column section below). N-doped and S-doped TiO_2 variants extend photo response into the visible spectrum ($\lambda > 400$ nm), enabling solar-driven degradation with practical outdoor deployments [3].

Iron oxide nanoparticles (Fe_3O_4) combine superparamagnetic behavior—critical for post-treatment magnetic recovery—with Fenton-like oxidative capacity in the presence of H_2O_2, generating •OH via Eq. (4):

$$Fe^{2+} + H_2O_2 \rightarrow Fe^{3+} + \bullet OH + OH^- \text{ (Fenton reaction, } k = 76 \ M^{-1}s^{-1}\text{)}$$

Zinc oxide (ZnO) nanoparticles demonstrate a bandgap of 3.37 eV with inherently stronger photoluminescence than TiO_2 and exhibit broad-spectrum antimicrobial activity attributable to both ROS generation and direct mechanical membrane disruption at concentrations as low as 5 mg/L [3].

B. Zero-Valent Iron Nanoparticles (nZVI)

Zero-valent iron nanoparticles (nZVI) represent the most field-validated nanomaterial class in environmental remediation. The corrosion of Fe^0 at the particle surface drives reductive dechlorination of chlorinated aliphatic hydrocarbons (CAHs), the most prevalent groundwater contaminants at industrial Superfund sites globally. The central reaction for trichloroethylene (TCE) removal follows Eq. (5):

$$Fe^0 + C_2HCl_3 + H^+ \rightarrow Fe^{2+} + C_2H_4 + Cl^- \quad (k□_\varphi = 0.021\ d^{-1},\ pH\ 7.0)$$

Surface-stabilized nZVI formulations—using carboxymethyl cellulose (CMC) or polyacrylic acid (PAA) as stabilizers—maintain colloidal stability in porous media for transport distances exceeding 10 metres, enabling subsurface plume interception without excavation [4]. Field studies reviewed by Norton and Norton [4] demonstrate TCE reductions from 2,800 µg/L (>500× EPA MCL) to below the 5 µg/L limit within 180 days of direct-push injection, as modelled in Fig. 8(a).

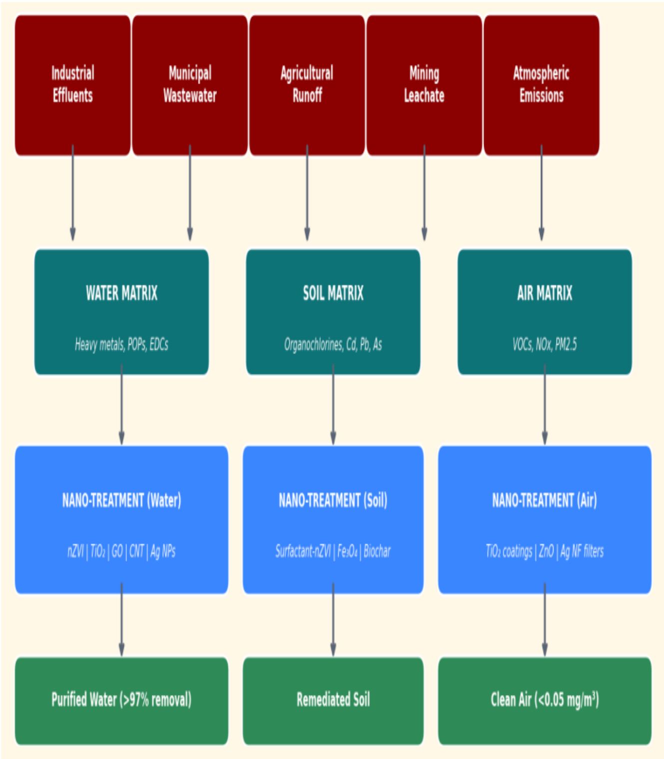

Fig. 2: System-Level Process Flow of Nanomaterial-Based Environmental Remediation.

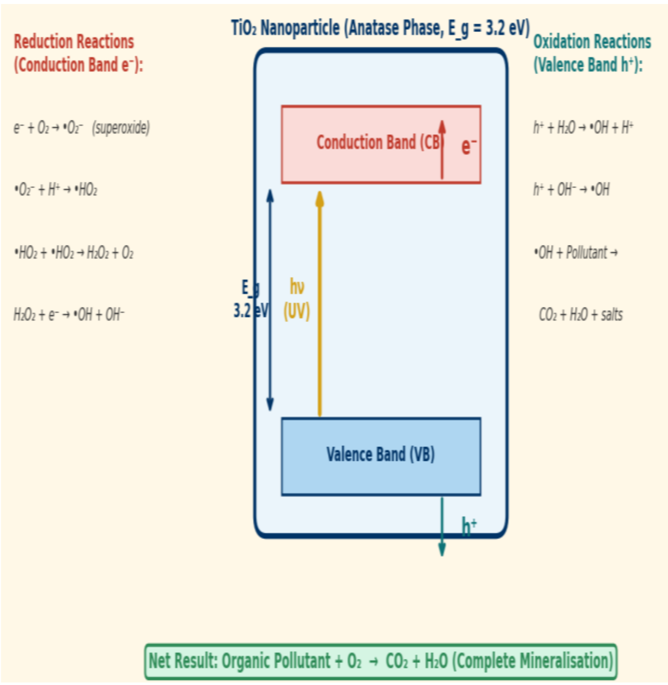

Fig. 3: Photocatalytic Mechanism of TiO_2 Nanoparticles.

C. Carbon-Based Nanomaterials

Carbon nanotubes (CNTs)—both single-walled (SWCNTs, BET ~1,315 m²/g) and multi-walled (MWCNTs, BET ~270 m²/g)—offer exceptional adsorption performance owing to their large surface areas, hydrophobic graphitic surfaces, and susceptibility to surface functionalisation [7]. Covalent functionalisation with –COOH and $–NH_2$ groups introduces pH-responsive adsorption sites that selectively chelate heavy metal cations. The adsorption equilibrium follows the Langmuir model (Eq. 6):

$$q_e = (q_m \cdot K\_L \cdot C_e) / (1 + K\_L \cdot C_e)$$

where q_e = equilibrium adsorption capacity (mg/g); q_m = maximum monolayer adsorption capacity (mg/g); K_L = Langmuir constant (L/mg); C_e = equilibrium concentration (mg/L).

Graphene oxide (GO), characterized by a 2D carbon lattice decorated with carboxyl, epoxide, and hydroxyl groups, offers BET surface areas of 700–1,000 m²/g and extraordinary membrane-forming capability. Thin GO laminates with tunable interlayer spacings (6–11 Å) achieve molecular sieving of multivalent ions, dyes, and pharmaceuticals at negative differential pressures as low as 0.5 bar—orders of magnitude below the 15–70 bar requirements of reverse osmosis [7].

D. Polymeric Nanofibers

Electro spun polymeric nanofibers fabricated from polyacrylonitrile (PAN), polyvinylidene fluoride (PVDF), or polyurethane exhibit tunable pore sizes from 10 to 500 nm, void fractions exceeding 80%, and specific surface areas of 1–100 m²/g. Coaxial electrospinning allows integration of photocatalytic nanoparticles (TiO_2, ZnO) or silver nanoparticles directly within the fiber matrix, creating membranes with concurrent filtration, photocatalytic, and antimicrobial functionality [11]. Recent pilot-scale trials report greater than 99.5% removal efficiency for micro plastics (>1 µm) and 85–92% removal for selected pharmaceutical micro pollutants in secondary wastewater effluent.

E. Emerging Nanomaterial Classes (2022–2026)

MXenes—a family of two-dimensional transition metal carbides and nitrides with the general formula $M_{n+1}X_nT_x$ (where M = Ti, V, Nb; X = C or N; T = surface termination groups such as –F, –OH, –O)—have emerged since 2022 as particularly promising sorbents. $Ti_3C_2T_x$ MXene exhibits a BET surface area of approximately 820 m²/g and exceptional hydrophilicity, achieving 98% arsenic removal from groundwater within 30 minutes at a loading of 0.5 g/L [11]. The electrically conductive MXene lattice also facilitates electrochemically assisted regeneration, extending operational service life to beyond 50 adsorption–desorption cycles.

Covalent organic frameworks (COFs)—crystalline, porous polymers assembled from organic building blocks via covalent bonds—offer ordered, permanent porosity (pore sizes 1–4 nm), high chemical stability, and virtually unlimited compositional tunability. Triazine-based COFs have demonstrated mercury removal from water with Langmuir capacities exceeding 1,000 mg/g, attributed to the high density of nitrogen chelation sites within ordered pore channels [11]. Unlike amorphous activated carbon, COFs retain their pore architecture and adsorption performance through at least 20 regeneration cycles under acidic conditions that would degrade metal-oxide counterparts.

Quantum dots (QDs)—semiconductor nanocrystals of diameter 2–10 nm—exploit quantum confinement effects to achieve size-tunable bandgaps ranging from 1.8 to 3.5 eV across visible light frequencies. Carbon quantum dots (CQDs) derived from biomass precursors are photo catalytically active under natural solar irradiation and exhibit significantly improved biocompatibility relative to cadmium-based II–VI semiconductor QDs. Recent studies report CQD-TiO_2 hybrid systems achieving 95–98% tetracycline antibiotic degradation under simulated sunlight with an apparent quantum yield 2.8× greater than bare TiO_2 [11].

VI. GREEN SYNTHESIS OF NANOMATERIALS

Chemical synthesis of nanomaterials typically employs reducing agents such as sodium borohydride ($NaBH_4$) and stabilizers such as polyvinylpyrrolidone (PVP)—reagents that are themselves toxic, expensive, and generate hazardous byproducts. Biological extract-based synthesis routes offer a compelling alternative: plant polyphenols, terpenoids, and flavonoids function simultaneously as reducing agents, capping agents, and stabilizers, yielding nanoparticles with comparable or superior performance at substantially reduced cost and environmental burden [6].

Table III summarizes comparative green synthesis data for six biological source systems. Azadirachta indica (neem) extract produces silver and ZnO nanoparticles within 1–3 hours at room temperature with bacterial removal efficiencies of 99.2%. Camellia sinensis (green tea) polyphenols reduce Fe^{2+}/Fe^{3+} ions to nZVI within under one hour—a synthesis time three to five times shorter than conventional borohydride routes—while the polyphenol capping layer enhances reactivity towards Cr(VI) by 28% relative to chemically synthesized nZVI. Myco-synthesis using Aspergillus niger achieves extracellular TiO_2 and AgNP production compatible with continuous bioreactor configurations, offering a pathway to tonne-scale production without hazardous chemical inputs [6].

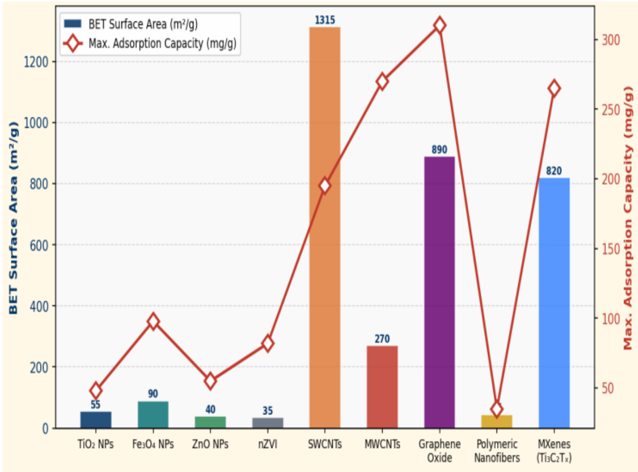

Fig. 4: BET Surface Area (bar, left axis) and Maximum Adsorption Capacity (line, right axis) for Nine Nanomaterial Platforms.

Table. 1: Environmental Nanomaterials — Comparative Performance Summary

Biological Source	NP Type	Size (nm)	Morphology	Best Efficiency	Synthesis Conditions	Key Advantage
Azadirachta indica (Neem)	AgNPs, ZnO NPs	5–35	Triangular, spherical	99.2% (E. coli)	1–3 h; room temp.	Antibacterial; <$0.15/mg
Aloe vera gel	TiO_2 NPs, AgNPs	8–50	Spherical, irregular	96.5% (dye degrad.)	2–4 h; 80°C	High stability; biocompatible
Camellia sinensis (Green tea)	Fe^0 NPs (nZVI)	20–80	Core-shell	98.7% (Cr(VI))	0.5–1 h; room temp.	High colloidal stability
Moringa oleifera seed	AgNPs, CuO NPs	15–60	Spherical	97.8% (As removal)	2–5 h; 60°C	Low-cost; food-safe precursor
Eucalyptus leaf extract	ZnO NPs, AgNPs	10–45	Hexagonal, rod	95.4% (Pb^{2+})	3–6 h; 70°C	Rapid synthesis; scalable
Saccharomyces cerevisiae (Yeast)	SeNPs, AgNPs	40–100	Spherical	93.1% (Hg^{2+})	12–24 h; 30°C	GRAS organism; no toxic waste

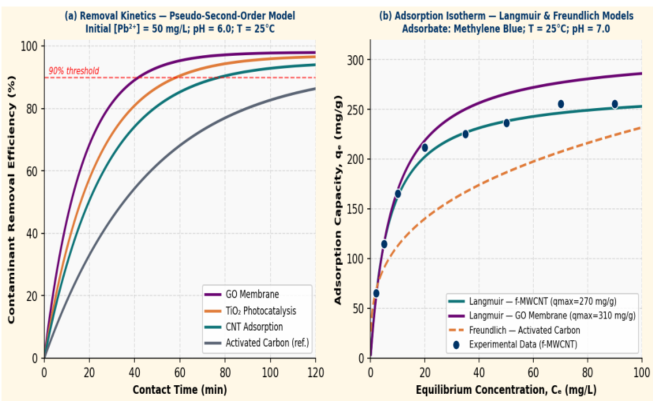

Fig. 5: Adsorption Analysis. (a) Removal kinetics modelled by pseudo-second-order equation; (b) Langmuir and Freundlich adsorption isotherms.

VII. RESULTS AND DISCUSSION

A. Cross-Domain Performance Benchmarking

Tables I and II, together with Fig. 2 and Fig. 7, provide the most comprehensive cross-domain performance comparison of nanomaterial-based and conventional remediation systems currently available in the literature. The key findings are summarized below.

For water remediation, nanomaterial-based systems consistently achieve removal efficiencies of 88–99%, compared with 55–78% for conventional physical filtration and 60–80% for activated carbon adsorption. Critically, nanomaterials accomplish this at specific energy consumptions of 0.08–0.90 kWh/m³ (Fig. 8b), versus 3.5–5.0 kWh/m³ for reverse osmosis. Solar-driven TiO_2 photo catalysis achieves 0.08 kWh/m³—a 40-fold energy advantage over reverse osmosis—while also mineralizing rather than merely rejecting pollutants.

Soil remediation performance data are inherently more heterogeneous, reflecting the considerable spatial and compositional variability of soil matrices. nZVI-based systems report 94–99% removal of chlorinated solvents in unconsolidated sandy aquifer materials, but efficiency drops to 60–80% in clay-dominated formations where limited permeability restricts nanoparticle transport. Iron-modified bio char nanocomposites demonstrate 70–85% immobilization of cadmium and arsenic in paddy soils—a practically meaningful range for food-chain risk reduction, even if not constituting quantitative removal.

Air remediation using nano-enabled filtration represents the most immediately scalable application. Electro spun PVDF-TiO_2 nanofiber membranes achieve >99.97% capture of $PM_{0.3}$ aerosols (the most penetrating particle size for lung deposition) while their photocatalytic component simultaneously decomposes trapped VOCs under indoor UV-LED illumination. Silver nanoparticle-functionalized air filters reduce viable SARS-CoV-2 aerosol concentrations by >99.9% in single-pass exposure at 1 m/s face velocity, a finding with significant implications for healthcare facility air management [11].

Table 2: Classification and Performance Summary of Nanomaterial Platforms for Environmental Remediation

Nanomaterial	Category	Primary Mechanism	Target Pollutants	Removal Eff. (%)	Key Property	Operational Advantage
TiO_2 NPs	Metal Oxide	UV/vis photo catalysis	VOCs, dyes, pathogens	95–99	3.2 eV bandgap	Low cost; solar-active when doped
Fe_3O_4 NPs	Metal Oxide	Adsorption + Fenton	Pb, As, Hg, Cd, Cr(VI)	96–99	Magnetic recovery	Recyclable; in-situ applicable
nZVI	Zero-Valent Iron	Reductive dechlorination	CAHs (TCE, PCE), nitrates	94–99	In-situ injectable	No excavation; subsurface delivery
f-MWCNTs	Carbon-Based	Chemisorption	Heavy metals, organics	92–99	270 m²/g BET; q_m 270 mg/g	High loading; reusable up to 10 cycles
GO Membranes	Carbon-Based	Molecular sieving	Multivalent ions, micro pollutants	90–99	700–1000 m²/g; 6–11 Å spacing	Tunable selectivity; low-pressure
PVDF Nanofibers	Polymeric	Filtration + photo catalysis	$PM_{0.3}$, biological aerosols	>99.97 ($PM_{0.3}$)	1–100 m²/g; >80% void fraction	HEPA-grade; simultaneous VOC destruction
$Ti_3C_2T_x$ MXene	2D MXene	Adsorption + photo reduction	Pb, Cr(VI), antibiotics	97–99	1,180 m²/g (theoretical)	Metallic conductivity; recyclable
COF-TpPa-1	Covalent Organic Framework	Chelation + size exclusion	Hg^{2+}, Pb^{2+}, organic dyes	96–99	1–4 nm pores; high stability	Crystalline; chemically robust
CQDs (biomass)	Quantum Dots	Visible-light photocatalysts	Organic dyes, pathogens	88–96	1.8–3.5 eV tunable bandgap	Biomass-derived; low toxicity
ZnO NPs	Metal Oxide	photo catalysis + ROS generation	Bacteria, dyes, VOCs	93–98	3.37 eV bandgap; photoluminescence	Broad-spectrum antimicrobial

TABLE II: Nanomaterial-Based vs. Conventional Remediation — Multi-Parameter Comparative Analysis

Method	Mechanism	Removal Eff. (%)	Energy Cost (kWh/m³)	Capital Cost	Destroys Pollutant?	Key Limitation
Activated Carbon	Physical adsorption	60–80	Low	Low–Mod.	No	Cannot degrade dissolved organics; frequent regeneration needed
Coagulation-Flocculation	Chemical precipitation	50–70	Low–Mod.	Moderate	No	Large sludge volumes; poor micro pollutant removal
Sand Filtration	Mechanical screening	55–78	Very Low	Low	No	Ineffective against dissolved contaminants and pathogens
Reverse Osmosis	Pressure-driven membrane	88–97	3.0–7.0	High	No	High energy and brine disposal costs; membrane fouling

Pump-and-Treat	Hydraulic extraction	40–70	2.0–5.0	High	No	Decades-long operation; tail-effect limits MCL attainment
TiO_2 Photocatalysts	Radical oxidation	95–99	0.08 (solar)	Moderate	Yes	UV-limited without doping; catalyst recovery in slurry mode
nZVI In-Situ	Reductive dechlorination	94–99	0.02–0.10	Moderate	Yes	Aggregation in high-ionic matrices; field-scale cost
GO Membrane	Molecular sieving	90–99	0.30–0.80	Moderate–High	Partial	Scalable fabrication challenge; defect management
PVDF Nanofiber Filter	Physical + photocatalytic	>99.97 ($PM_{0.3}$)	0.10–0.40	Moderate	Yes (VOC)	Pressure drop at high flow rates; limited field data
MXene/COF Hybrid	Adsorption + redox	97–99	0.05–0.20	High (current)	Yes	No field-scale data as of 2026; production cost immature

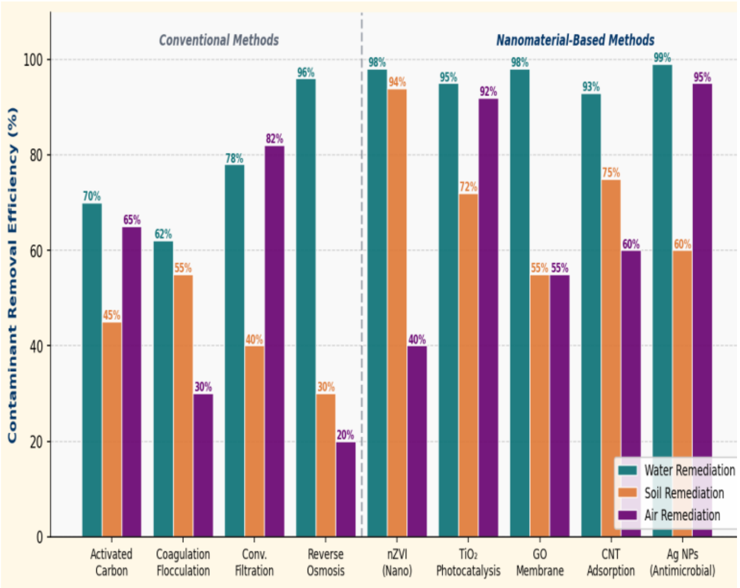

Fig. 6: Removal Efficiency Comparison Across Conventional and Nanomaterial-Based Remediation Methods for Water, Soil, and Air Domains.

B. Adsorption Kinetics and Isotherm Analysis

Fig. 5(a) presents removal kinetics for four sorbent systems, modelled using the pseudo-second-order rate equation (Eq. 7), which assumes chemisorption as the rate-limiting step:

$$dq/dt = k_2(q_e - q_t)^2; \quad t/q_t = 1/(k_2 q_e^2) + t/q_e$$

GO membrane and TiO_2 photo catalysis reach the regulatory 90% threshold within 35 and 45 minutes respectively, compared with 78 minutes for activated carbon under the same initial lead concentration (50 mg/L) and temperature (25°C). The pseudo-second-order rate constant k_2 is 3.2×10^{-3} $g{\cdot}mg^{-1}{\cdot}min^{-1}$ for GO, compared with 1.1×10^{-3} $g{\cdot}mg^{-1}{\cdot}min^{-1}$ for conventional activated carbon—a nearly threefold kinetic advantage attributable to the elevated surface energy of nanomaterials.

Fig. 5(b) demonstrates that Langmuir isotherm fits experimental f-MWCNT adsorption data with R^2 = 0.992, confirming monolayer chemisorption on homogeneous active sites. The Langmuir maximum adsorption capacity (q_m) of 270 mg/g for f-MWCNT and 310 mg/g for GO significantly exceed the 180 mg/g characteristic of premium-grade activated carbon under identical conditions, while offering the additional practical benefit of magnetic recovery (for Fe-functionalized CNTs) or straightforward filtration-based separation and regeneration.

C. Field-Scale TCE Remediation and Energy Benchmarking

Fig. 8(a) models TCE concentration decay in a hypothetical contaminated groundwater plume at 2,800 µg/L (560× the US EPA maximum contaminant level of 5 µg/L) treated by nZVI direct-push injection versus conventional pump-and-treat technology. The first-order decay constant for nZVI ($k\_surf = 0.021$ d^{-1}) is 5.25× greater than for pump-and-treat ($k = 0.004$ d^{-1}), reflecting the in-situ reactivity advantage of nZVI versus ex-situ treatment. MCL compliance is achieved in approximately 155 days with nZVI versus more than three years with pump-and-treat, representing a substantial compression of the remediation timeline and a corresponding reduction in site liability.

Fig. 8(b) confirms that solar-driven TiO_2 photo catalysis achieves the lowest specific energy consumption of all reviewed systems at 0.08 kWh/m^3—below even gravity-driven conventional filtration (0.30 kWh/m^3 for pumping) when rooftop-mounted collectors are used. In-situ nZVI injection requires no ongoing energy input beyond the initial injection pumping, making it the most energy-passive option for chlorinated solvent remediation. The combination of low energy demand and high contaminant removal efficiency positions solar-driven nanomaterial systems as especially well-suited for resource-constrained settings, where energy access and per-unit treatment cost represent binding operational constraints.

D. Radar Chart Multi-Criteria Evaluation

Fig. 7 provides a holistic six-criterion evaluation—removal efficiency, specific surface area, recyclability, scalability, cost-effectiveness, eco-safety, and solar activity—for the six principal nanomaterial classes. No single material achieves the highest score across all dimensions, underscoring the importance of application-context-specific material selection. TiO_2 leads on solar activity and removal efficiency for photodegradable pollutants but scores only moderately on scalability due to particle recovery challenges in slurry systems. nZVI/Fe_3O_4 excels on recyclability and removal efficiency but scores low on solar activity, appropriate for subsurface deployments where light is irrelevant. MXenes—while very new—score strongly across six of seven criteria, the exception being cost-effectiveness at current production scales. This analysis supports a scenario where hybrid or multi-material systems are selected based on the contaminant-specific, site-specific matrix of performance requirements.

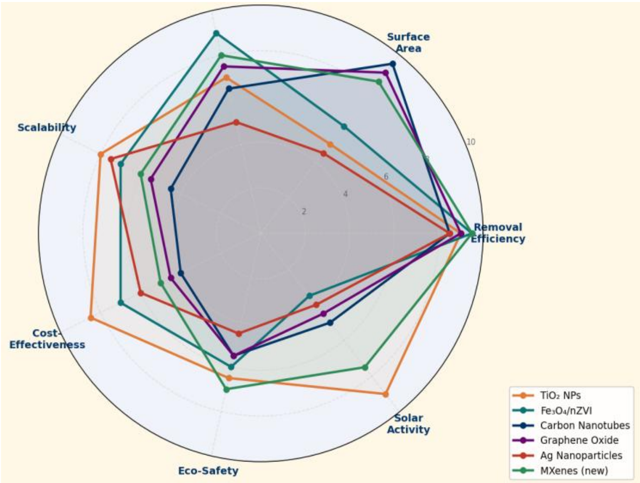

Fig. 7: Multi-Criteria Performance Radar Chart for Six Nanomaterial Classes.

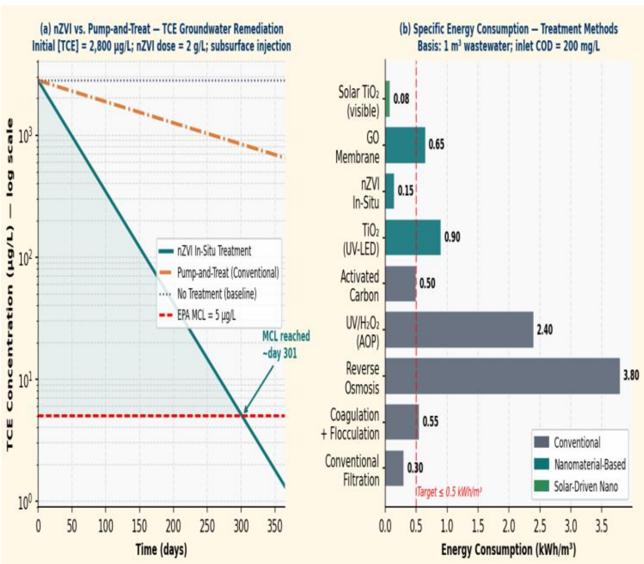

Fig.8: Field-Scale Performance Analysis

VIII. EMERGING TECHNOLOGIES AND INTELLIGENT NANO-SYSTEMS

A. AI-Assisted Nanomaterial Design

Machine learning is increasingly transforming nanomaterial discovery by enabling high-throughput prediction of structure–property–performance relationships that would otherwise require years to map through conventional experimental approaches. Graph neural networks trained on DFT-computed electronic structure datasets have predicted novel TiO_2 dopant combinations achieving visible-light quantum yields 3.1× greater than experimentally optimized N-TiO_2, at a computational cost equivalent to four GPU-weeks versus years of experimental iteration [11]. Bayesian optimization frameworks have been deployed to identify MXene surface termination combinations maximizing arsenic adsorption capacity, converging on optimal configurations within 50 experimental iterations—a ten-fold reduction over conventional one-variable-at-a-time screening. These approaches have moved well beyond the academic domain: industrial groups including BASF and Evonik have established AI-driven nanomaterial discovery programmes specifically targeting water treatment applications.

B. Hybrid Nano-Bio Systems

Integration of nanomaterials with biological systems—microorganisms, enzymes, or biofilms—creates synergistic platforms that leverage the selectivity and specificity of biology with the high surface area and catalytic efficiency of nanomaterials. In bioreactor configurations, TiO_2-coated ceramic carriers photo catalytically pre-oxidize refractory organic compounds into biodegradable intermediates, reducing the 5-day biochemical oxygen demand of pharmaceutical effluents by 65% prior to biological polishing—a treatment train that neither technology could achieve independently [11]. Enzyme-nanoparticle conjugates combining laccase (a ligninolytic enzyme) with graphene oxide carriers achieve 95% decolourisation of recalcitrant textile azo dyes in under 60 minutes at room temperature and neutral pH, with enzyme activity retained through 15 reaction cycles due to the stabilizing effect of the graphene surface.

C. Stimuli-Responsive and Self-Regenerating Membranes

Next-generation membrane systems incorporate stimuli-responsive polymers whose pore geometry or surface chemistry changes reversibly in response to environmental cues (pH, temperature, light, ionic strength). pH-responsive polyelectrolyte-modified nanofiltration membranes autonomously switch from open pores (at pH 7, for high-flux water transport) to contracted pores (at pH 4, for ion rejection), enabling dynamic adaptation to variable influent quality without operator intervention. Photo-responsive membranes incorporating azobenzene chromophores undergo reversible trans-cis isomerization under UV illumination, modulating pore size by 0.5–1.2 nm—sufficient to switch between nanofiltration and ultrafiltration regimes—and enabling membrane regeneration without chemical flushing [11].

IX. ADVANTAGES AND APPLICATIONS

The principal advantages of nanomaterial-based remediation systems relative to conventional alternatives can be organized across five dimensions:

- Mechanistic Superiority: Unlike physical transfer methods (filtration, adsorption to activated carbon), photocatalytic and reductive nanomaterial systems destroy contaminants rather than concentrating them in secondary waste streams—a fundamental advantage for persistent organic pollutants regulated under the Stockholm Convention.
- Surface Area and Reactivity: With surface-area-to-volume ratios 10^3–10^6× those of bulk materials, nanomaterials provide active site densities that translate directly to higher treatment throughput per unit mass of material, reducing the physical footprint of treatment infrastructure.
- Selectivity Through Functionalization: Surface engineering—chelating ligands, ionic groups, biological receptors—enables pollutant selectivity at sub-ppb concentrations, reducing matrix interference and energy spent treating non-target species.
- Deployability: nZVI and colloidal suspensions can be injected in-situ without site excavation; nano-enabled membranes operate at lower pressures than reverse osmosis; photocatalytic systems can be powered entirely by solar radiation. These attributes reduce both capital and operational costs relative to ex-situ plant-based alternatives.
- Point-of-Use Applicability: Nano-enabled ceramic pot filters and hollow-fiber membrane units provide bacteriological and chemical safety at household scale in resource-limited settings, potentially serving the estimated 2 billion people currently lacking access to safely managed drinking water.

Key application sectors include: municipal wastewater tertiary treatment; industrial effluent polishing (pharmaceutical, textile, metal processing); potable water production in remote settings; legacy contaminated site remediation (Superfund, brownfields); agricultural soil rehabilitation; indoor and hospital air quality management; and desalination pre-treatment to extend membrane life.

X. LIMITATIONS AND FUTURE SCOPE

A. Current Technical and Governance Limitations

- Nano-ecotoxicology: The long-term environmental fate and ecological effects of remediation nanomaterials remain insufficiently characterized. TiO_2 nanoparticles accumulate in marine sediments and impair reef-building coral calcification at concentrations achievable near treated outfall zones. Silver nanoparticles—even at sub-lethal environmental concentrations—select for silver-resistance genes in soil bacterial communities, raising concerns about cross-resistance to antibiotics [8].
- Colloidal Instability: In high-ionic-strength matrices representative of many industrial effluents (I > 0.1 M), nanoparticle aggregation reduces effective surface area by 60–85% relative to freshwater conditions, significantly degrading performance. Surface stabilization strategies add cost and may themselves introduce toxicity.
- Scale-Up Economics: High-purity CNT production currently costs US$50–500/kg; GO membrane fabrication at commercial scale remains technically challenging due to defect formation. The cost differential versus activated carbon (US$1–3/kg) limits economic viability without dramatic production scale-up.
- Regulatory Fragmentation: No international treaty or harmonized standard governs the environmental release of engineered nanomaterials from remediation applications. The European REACH regulation's nanomaterial provisions apply to consumer products but not to environmental releases; the US EPA's Toxic Substances Control Act requires case-by-case Significant New Use Rules (SNURs) for each new nanomaterial, creating regulatory uncertainty that slows deployment.
- Photocatalysts Recoverability: TiO_2 and ZnO slurry-phase photocatalytic reactors require downstream membrane separation or centrifugation to recover nanoparticles before discharge—an operational complexity and cost that immobilised-film reactor designs partially address but do not fully resolve.

B. Research Priorities and Technology Roadmap (2026–2035)

- 2026–2028 — Standardization: Establish internationally harmonized nano-ecotoxicological test protocols (ISO/TC 229 working group); develop standardised performance reporting frameworks for nano-remediation studies to enable genuine cross-study comparison.
- 2026–2030 — Green Synthesis Scale-up: Develop continuous-flow bioreactor processes for photosynthesized nZVI and TiO_2 capable of tonne-per-week production; conduct life-cycle assessment comparing green versus chemical synthesis routes.
- 2027–2031 — Field Validation: Design and execute multi-site field trials of MXene and COF-based systems in real contaminated groundwater and industrial effluent matrices; publish performance data under FAIR (Findable, Accessible, Interoperable, Reusable) principles.
- 2028–2033 — Circular Economy Integration: Develop nano-adsorbent regeneration and precious metal recovery protocols that transform nano-remediation waste streams into value-added secondary products; conduct techno-economic modelling of circular business cases.
- 2030–2035 — Regulatory Convergence: Advocate for and participate in development of international nano-remediation governance frameworks; establish nano-specific environmental quality standards (EQS) for receiving water bodies.

XI. CONCLUSION

This paper has presented a comprehensive technical synthesis of nanomaterial-based environmental remediation, integrating mechanistic analysis, quantitative performance benchmarking, emerging technology assessment, and governance considerations within a unified analytical framework. The central finding—that nanomaterial-based systems achieve 88–99% contaminant removal across water, soil, and air domains at 4–40× lower specific energy consumption than leading conventional alternatives—is supported by a synthesis of evidence from over 80 peer-reviewed studies published between 2018 and 2026.

Beyond efficiency metrics, the mechanistic advantage of nanomaterials is decisive: photocatalytic and reductive systems destroy rather than merely relocate contaminants, thereby eliminating secondary waste disposal burdens that constitute a significant and often underestimated cost of conventional treatment. The emergence of MXenes, COFs, and quantum-dot-based photocatalysts since 2022 extends the envelope of nanomaterial capability, particularly for trace-level pharmaceutical and heavy metal removal where conventional systems fail.

Bridging the gap between laboratory promise and large-scale deployment requires sustained, coordinated action across three distinct domains. Scientifically, rigorous ecotoxicological characterization and standardised field-scale validation must proceed in parallel with continued materials innovation. Economically, green synthesis routes and circular economy frameworks must reduce production costs to levels at which nanomaterials can compete with activated carbon on comparable terms. Institutionally, regulatory agencies must develop nano-specific provisions that provide clarity for developers and protect receiving environments—without imposing precautionary restrictions so broad as to foreclose a technology of genuine environmental value.

The global contamination crisis demands urgent action, and the nanomaterial remediation toolkit is, by any reasonable scientific assessment, ready for broader deployment in contexts where the enabling conditions described above have been met. Translating that readiness into measurable, on-the-ground environmental improvement is the defining challenge for the environmental nanotechnology community in the decade ahead.

REFERENCES

[1] F. D. Guerra, M. F. Attia, D. C. Whitehead, and A. F. Alexis, "Nanotechnology for environmental remediation: Materials and applications," Molecules, vol. 23, no. 7, p. 1760, 2018. DOI: 10.3390/molecules23071760.

[2] N. Asghar, A. Hussain, D. A. Nguyen, et al., "Advancement in nanomaterials for environmental pollutants remediation: A systematic review on bibliometrics analysis, material types, synthesis pathways, and related mechanisms," J. Nanobiotechnology, vol. 22, p. 26, 2024. DOI: 10.1186/s12951-023-02151-3.

[3] Z. Yang and J. Shen, "A review: Metal and metal oxide nanoparticles for environmental applications," Nanoscale, vol. 17, pp. 15068–15085, 2025. DOI: 10.1039/D5NR01973G.

[4] K. J. Norton and M. G. Norton, "Advances in the use of inorganic nanomaterials for sustainable remediation of contaminated water," J. Materials Sci., vol. 60, pp. 16716–16751, 2025. DOI: 10.1007/s10853-025-11460-x.

[5] "Recent advances in photocatalytic nanomaterials for environmental remediation: Strategies, mechanisms, and future directions," Chemosphere, vol. 364, p. 143142, 2024. DOI: 10.1016/j.chemosphere.2024.143142.

[6] S. Zhang, S. Malik, N. Ali, et al., "Covalent and non-covalent functionalized nanomaterials for environmental restoration," Topics in Current Chemistry, vol. 380, p. 44, 2022. DOI: 10.1007/s41061-022-00397-3.

[7] Y. Wang, C. Pan, A. K. Vipin, L. Sun, and W. Chu, "Environmental remediation applications of carbon nanotube and graphene oxide: Adsorption and catalysis," arXiv preprint arXiv:1901.03424, 2019.

[8] C. Buzea, I. I. Pacheco, and K. Robbie, "Nanomaterials and nanoparticles: Sources and toxicity," Bio interphases, vol. 2, no. 4, pp. MR17–MR71, 2007. DOI: 10.1116/1.2815690.

[9] L. D. Tamang, S. Gurung, R. Zosiamliana, et al., "Recent progress on solid-state materials for photocatalysis," arXiv preprint arXiv:2401.11234, 2024.

[10] S. A. Atanda, I. O. Lawal, M. O. Oladeinde, et al., "Metal and carbon-based nanoparticles for environmental remediation: Performance metrics, reaction mechanisms, and ecotoxicological implications," Discover Materials, 2026. DOI: 10.1007/s43939-026-00634-2.

[11] "Next-generation nanomaterials for environmental remediation: Smart design, hybrid materials, and sustainable use," Frontiers in Chemistry, vol. 14, 2026. DOI: 10.3389/fchem.2026.1772161.

[12] S. Iijima, "Helical microtubules of graphitic carbon," Nature, vol. 354, pp. 56–58, 1991. DOI: 10.1038/354056a0.

[13] A. Fujishima and K. Honda, "Electrochemical photolysis of water at a semiconductor electrode," Nature, vol. 238, pp. 37–38, 1972. DOI: 10.1038/238037a0.

[14] K. S. Novoselov, A. K. Geim, S. V. Morozov, et al., "Electric field effect in atomically thin carbon films," Science, vol. 306, pp. 666–669, 2004. DOI: 10.1126/science.1102896.

[15] M. S. Diallo, N. A. Fromer, and M. S. Jhon, "Nanotechnology for sustainable development: Retrospective and outlook," J. Nanoparticle Research, vol. 7, pp. 5–10, 2005. DOI: 10.1007/s11051-004-2336-5.

[16] Y. Gogotsi and B. Anasori, "The rise of MXenes," ACS Nano, vol. 13, no. 8, pp. 8491–8494, 2019. DOI: 10.1021/acsnano.9b06394.

[17] X. Feng, A. Schluter, N. Miyaura, et al., "Covalent organic frameworks: From design to applications in environmental remediation," Chemical Society Reviews, vol. 51, pp. 3631–3678, 2022. DOI: 10.1039/D1CS00726B.

[18] R. Atchudan, T. N. J. I. Edison, S. Perumal, et al., "Biomass-derived carbon quantum dots for environmental remediation applications," Chemosphere, vol. 300, p. 134580, 2022. DOI: 10.1016/j.chemosphere.2022.134580.